Variant Ionotropic Glutamate Receptors as Chemosensory Receptors in *Drosophila*

Richard Benton,[1,3,4] Kirsten S. Vannice,[1,5] Carolina Gomez-Diaz,[1,6] and Leslie B. Vosshall[1,2,*]
[1]Laboratory of Neurogenetics and Behavior
[2]Howard Hughes Medical Institute
The Rockefeller University, 1230 York Avenue, Box 63, New York, NY 10065, USA
[3]Center for Integrative Genomics, Faculty of Biology and Medicine, University of Lausanne, CH-1015 Lausanne, Switzerland
[4]Present address: Center for Integrative Genomics, Faculty of Biology and Medicine, University of Lausanne, CH-1015 Lausanne, Switzerland
[5]Present address: National Vaccine Program Office, 200 Independence Avenue SW, Washington, DC 20201, USA
[6]Present address: Department of Functional Biology, Faculty of Medicine, University of Oviedo, 33071 Oviedo, Spain
*Correspondence: leslie@mail.rockefeller.edu

SUMMARY

Ionotropic glutamate receptors (iGluRs) mediate neuronal communication at synapses throughout vertebrate and invertebrate nervous systems. We have characterized a family of iGluR-related genes in *Drosophila*, which we name ionotropic receptors (IRs). These receptors do not belong to the well-described kainate, AMPA, or NMDA classes of iGluRs, and they have divergent ligand-binding domains that lack their characteristic glutamate-interacting residues. IRs are expressed in a combinatorial fashion in sensory neurons that respond to many distinct odors but do not express either insect odorant receptors (ORs) or gustatory receptors (GRs). IR proteins accumulate in sensory dendrites and not at synapses. Misexpression of IRs in different olfactory neurons is sufficient to confer ectopic odor responsiveness. Together, these results lead us to propose that the IRs comprise a novel family of chemosensory receptors. Conservation of IR/iGluR-related proteins in bacteria, plants, and animals suggests that this receptor family represents an evolutionarily ancient mechanism for sensing both internal and external chemical cues.

INTRODUCTION

Species as diverse as bacteria, plants, and humans have the capacity to sense small molecules in the environment. Chemical cues can transmit the presence of food, alarm signals, and messages from conspecifics that signify mating compatibility. Peripheral chemical recognition largely relies on membrane receptor proteins that interact with external ligands and convert this binding into intracellular responses. The vast majority of identified chemosensory receptors in multicellular organisms belong to the seven transmembrane domain G protein-coupled receptor (GPCR) superfamily, including odorant, gustatory, and pheromone receptors in mammals, birds, reptiles, amphibians, fish, and nematodes (Bargmann, 2006). Unicellular organisms also use GPCRs for chemoreception, such as the pheromone receptors in budding yeast (Dohlman, 2002).

Insects can detect a wide range of environmental chemicals: bitter, sweet, and salty tastants, odors, pheromones, humidity, carbon dioxide, and carbonated water (reviewed in Dahanukar et al., 2005; Bargmann, 2006; Vosshall and Stocker, 2007; Benton, 2008). Most of these chemosensory stimuli are recognized by members of two evolutionarily related insect-specific chemosensory receptor families, the odorant receptors (ORs) and gustatory receptors (GRs). These proteins contain seven predicted transmembrane domains but are evolutionarily unrelated to GPCRs (Vosshall et al., 1999; Benton et al., 2006; Wistrand et al., 2006) and adopt a distinct membrane topology (Benton et al., 2006; Lundin et al., 2007). Recent analysis has indicated that insect ORs function as odor-gated ion channels (Sato et al., 2008; Wicher et al., 2008), setting them mechanistically apart from metabotropic vertebrate ORs.

Comprehensive analysis of the expression of these receptors in the fruit fly, *Drosophila melanogaster*, has hinted at the existence of other types of insect chemosensory receptors (Couto et al., 2005; Yao et al., 2005). This is particularly apparent in the major olfactory organ, the third segment of the antenna, which bears three types of olfactory sensory hairs (sensilla): basiconic, trichoid, and coeloconic. All olfactory sensory neurons (OSNs) innervating basiconic and trichoid sensilla generally express one OR, along with the OR83b coreceptor (reviewed in Vosshall and Stocker, 2007). However, with the exception of *OR35a/OR83b*-expressing neurons (Yao et al., 2005), OSNs housed in coeloconic sensilla do not express OR83b or members of the *OR* or *GR* gene families (Scott et al., 2001; Couto et al., 2005; Yao et al., 2005). Nevertheless, electrophysiological analysis has revealed the existence of multiple types of coeloconic OSNs tuned to acids, ammonia, and humidity (Yao et al., 2005), suggesting that other types of insect chemosensory receptors exist.

We previously carried out a bioinformatic screen for insect-specific genes with enriched expression in OSNs (Benton et al., 2007). Among these, we found members of a large expansion of the ionotropic glutamate receptor (iGluR) gene family of unknown biological function (Littleton and Ganetzky, 2000). Here, we provide evidence that these variant iGluRs represent a novel class of chemosensory receptor.

RESULTS

A Large Family of Divergent Ionotropic Glutamate Receptor-like Genes in *Drosophila*
From a bioinformatic screen for olfactory molecules (Benton et al., 2007), we identified six antennal-expressed genes encoding proteins annotated as iGluRs (data not shown) (Littleton and Ganetzky, 2000). Using these receptor sequences as queries, exhaustive BLAST searches of the *Drosophila* genome identified a family of 61 predicted genes and two pseudogenes. These genes are distributed throughout the genome, both as individual sequences and in tandem arrays of up to four genes (Figure 1A; data not shown). We named this family the ionotropic receptors (IRs) and assigned individual gene names to the *IR*s using nomenclature conventions of *Drosophila OR*s (*Drosophila Odorant Receptor Nomenclature Committee, 2000*) (Figure 1A).

Phylogenetic analysis of predicted IR protein sequences revealed that they are not closely related to members of the canonical families of iGluRs (AMPA, kainate, NMDA, or delta) (Figure 1B). However, they appear to have a similar modular organization to iGluRs, comprising an extracellular N terminus, a bipartite ligand-binding domain, whose two lobes (S1 and S2) are separated by an ion channel domain, and a short cytoplasmic C terminus (Figures 1 and 2 and data not shown) (Mayer, 2006). We note that the gene structure and protein sequence of most receptors are presently only computational predictions. Nevertheless, the family is extremely divergent, exhibiting overall amino acid sequence identity of 10%–70%. The most conserved region between IRs and iGluRs spans the ion channel pore (Figure 1C), suggesting that IRs retain ion-conducting properties.

The ligand-binding domains are considerably more variable, although alignment of small regions of the S1 and S2 lobes of IRs and iGluRs allowed examination of conservation in amino acid positions that make direct contact with glutamate or artificial agonists in iGluRs (Armstrong et al., 1998; Armstrong and Gouaux, 2000; Jin et al., 2003; Mayer, 2005) (Figure 2). Although all iGluRs have an arginine (R) residue in S1 that binds the glutamate α-carboxyl group, only 19 out of 61 (31%) IRs retain this residue (Figure 2A). In the first half of the S2 domain, nine out of 61 (15%) of IRs retain a threonine (T), which contacts the glutamate γ-carboxyl group in all AMPA and kainate receptors (Figure 2B). Interestingly, the iGluRs that lack this T residue (NR1, NR3A, delta) have glycine or serine and not glutamate as a preferred ligand (Mayer et al., 2006; Naur et al., 2007). Finally, in the second half of the S2 domain, 100% of the iGluRs have a conserved aspartate (D) or glutamate (E) that interacts with the α-amino group of the glutamate ligand, compared with ten out of 61 (16%) IRs (Figure 2B). Of 61 IRs, only three (IR8a, IR75a, IR75c) retain the R, T, and D/E residues characteristic

of iGluRs, although these residues lie within a divergent structural backbone. Other IRs have a diversity of different amino acids at one or more of these positions. Thus, the ligand-binding specificity of most or all IRs is likely to be both distinct from that of iGluRs and varied within the IR family.

IRs Are Expressed in Chemosensory Neurons that Do Not Express ORs or OR83b
We determined the expression of the *IR* family by both tissue-specific RT-PCR and RNA in situ hybridization. Fifteen *IR* genes are expressed in the antenna (Figure 1A and Figure 3). Transcripts of these genes were not detected elsewhere in the adult head, body, or appendages, except for *IR25a* and *IR76b*, which are also expressed in the proboscis (data not shown). Expression of the remaining 46 *IR* genes was not reproducibly detected in any adult tissue. It is unclear whether these genes are not expressed, expressed at different life stages, or expressed at levels below the detection threshold of our assays.

We analyzed where in the antenna *IR* genes are expressed compared to *OR*s by double RNA in situ hybridization with probes for the OR coreceptor *OR83b* and one of several *IR* genes, including *IR64a*, *IR76b*, *IR31a*, and *IR40a* (Figure 3A and data not shown). *IR*s are not expressed in basiconic and trichoid sensilla, as they are not coexpressed with *OR83b*, and *IR* expression persists in mutants for the proneural gene *absent md neurons and olfactory sensilla* (*amos*), which completely lack these sensilla types (Goulding et al., 2000; zur Lage et al., 2003) (Figure 3A, top and middle panels; data not shown). However, expression of these *IR*s is dependent upon the proneural gene *atonal*, which specifies the coeloconic sensilla as well as a feather-like projection called the arista, and a three-chambered pocket called the sacculus (Figure 3A, bottom panel; data not shown) (Gupta and Rodrigues, 1997; Jhaveri et al., 2000). Thus, *OR*s and *IR*s are expressed in developmentally distinct sensory lineages in the antenna. One exception is the subpopulation of coeloconic OSNs that expresses both *IR76b* and *OR35a/OR83b* (Couto et al., 2005; Yao et al., 2005) (Figure 3A). We confirmed that *IR*-expressing cells in the antenna are neurons by demonstrating that they coexpress the neuronal marker *elav* (Figure 3B and data not shown).

We next generated a comprehensive map of *IR* expression (Figures 3C–3F). Each *IR* was observed to have a topologically defined expression pattern that is conserved across individuals of both sexes (data not shown). *IR8a* and *IR25a*, which encode closely related receptors (Figure 1B), are broadly expressed, detected in overlapping populations of neurons around the sacculus and in the main portion of the antenna (Figure 3C; data not shown). *IR25a* but not *IR8a* is also detected in the arista (data not shown; see below). *IR21a* is expressed in approximately six neurons in the arista (Figure 3D), as well as five to ten neurons near the third chamber of the sacculus (Figure 3E, bottom panel). Three *IR*s display specific expression in neurons surrounding the sacculus: *IR40a* and *IR93a* are coexpressed in 10–15 neurons adjacent to the first and second sacculus chambers (Figure 3E, top panel), while *IR64a* is found in 10–15 neurons surrounding the third chamber (Figure 3E, middle panel).

The remaining nine *IR*s are expressed in coeloconic OSNs distributed across the antenna (Figure 3F). Double and triple
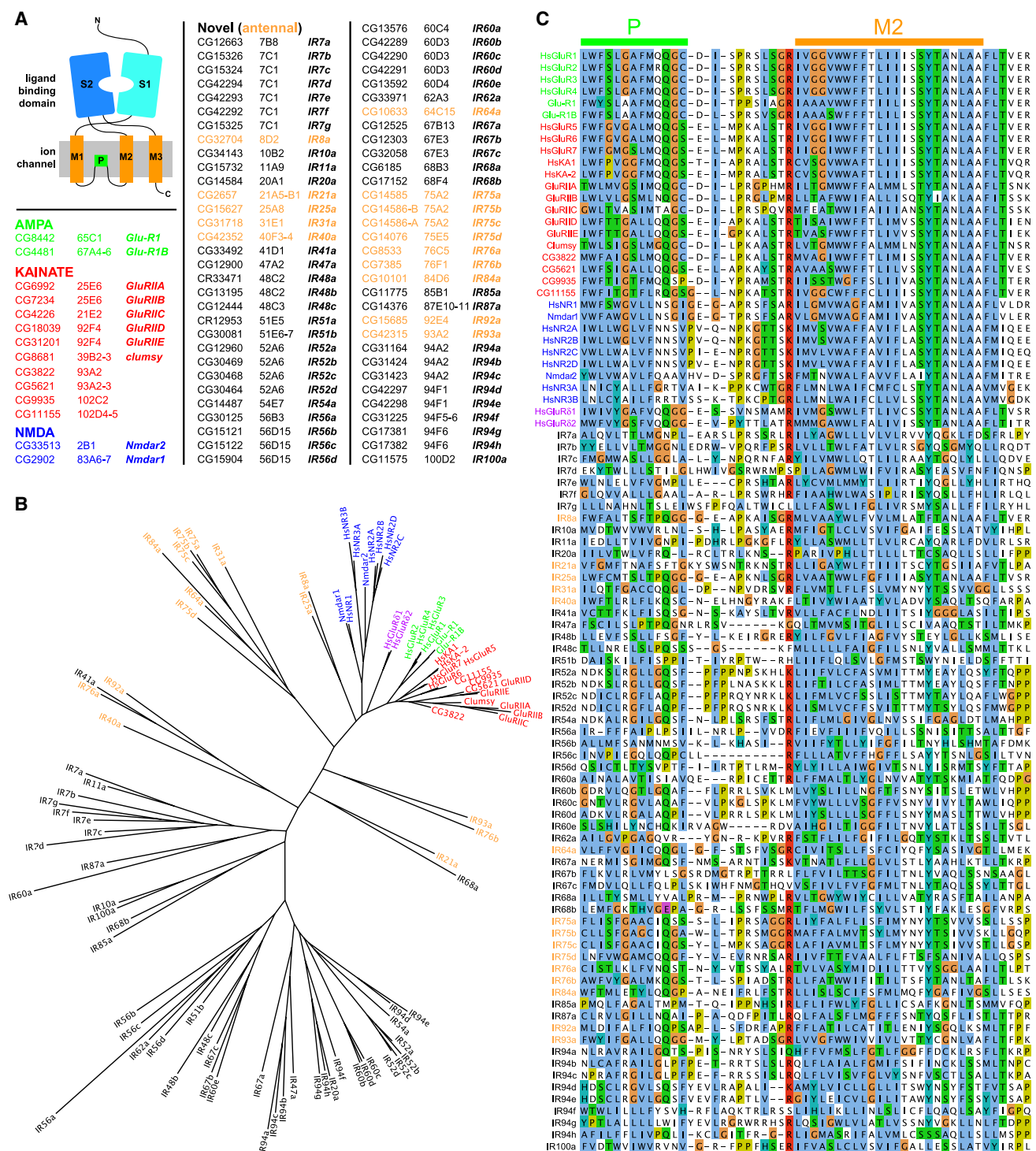
Figure 1. A Family of Divergent Ionotropic Glutamate Receptors in *Drosophila*

(A) Top left: model of iGluR domain organization. Bottom left and right: table of *Drosophila* iGluRs and IRs, with cytological locations and gene names.

(B) Phylogenetic tree of *Drosophila* and human iGluRs and *Drosophila* IRs, color-coded as in (A).

(C) Alignments of the amino acid sequences of *Drosophila* and human iGluRs and *Drosophila* IRs of part of the pore loop (P) and M2 transmembrane segment of the ion channel domain.
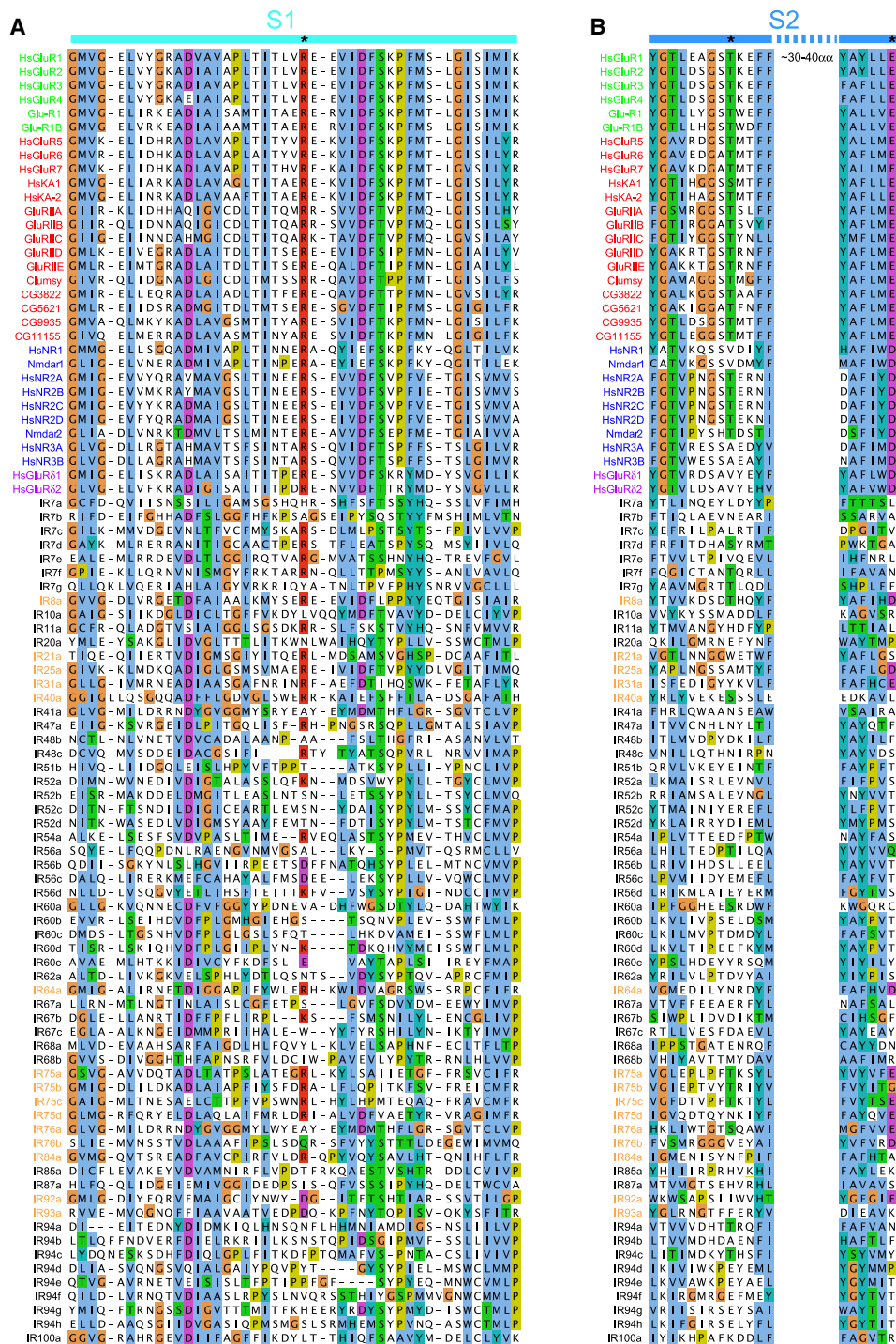
Figure 2. Ligand Binding Domains in Most IRs Lack Glutamate-Interacting Residues
ClustalW amino acid alignments of part of the S1 (A) and S2 (B) ligand binding domains of *Drosophila* and human iGluRs and *Drosophila* IRs. The positions of key ligand binding residues in iGluRs are marked with asterisks at the top.

RNA in situ hybridization revealed that individual neurons express between one and three different *IR* genes and are organized into specific clusters of two or three neurons. Four distinct clusters (cluster A–cluster D), containing two (cluster C) or three (clusters A, B, and D) neurons, could be defined by their expression of stereotyped combinations of *IR* genes (Figure 3F). Cluster C includes a coeloconic neuron that expresses *OR35a* and *OR83b* in addition to *IR76b*. Although each cluster is distinct,

there is overlap between the *IR*s they express. *IR76b* is expressed in one neuron in all four clusters, *IR75d* in three clusters, and *IR75a* in two clusters (Figures 3B and 3F). In addition to these selectively expressed receptors, individual neurons are likely to express one or both of the broadly expressed *IR8a* and *IR25a* genes (Figure 3C). The combinatorial expression patterns of the IRs raise the possibility that these genes define specific functional properties of these neurons.

Integration of Molecular and Functional Maps of the Coeloconic Sensilla

Our definition of four distinct clusters of *IR*-expressing neurons in the antenna (Figure 3F) is consistent with the identification of four types of coeloconic sensilla, named ac1–ac4, which have distinct yet partially overlapping sensory specificities (Yao et al., 2005). To examine whether *IR* expression correlates with the chemosensory properties of these OSNs, we compared the spatial organization of *IR*-expressing neurons using probes for unique *IR* markers for each cluster type to these functionally distinct sensilla types (Figure 4). As we lack a unique molecular marker for cluster B, this cluster was defined as those containing *IR75a*-expressing OSNs (present in cluster B and cluster C) that are not paired with *OR35a*-expressing cluster C neurons (Figure 4A). We found that each cluster has a different, though overlapping, spatial distribution in the antenna (Figure 4A). For example, cluster A neurons (marked by *IR31a*) are restricted to a zone at the anterior of the antenna, just below the arista, whereas cluster C neurons (marked by *IR75b*) are found exclusively in the posterior of the antenna. These stereotyped *IR* neuron distributions were observed in antennae from over 20 animals.

The initial description of the coeloconic sensilla classes did not describe their spatial distribution (Yao et al., 2005). We therefore recorded odor-evoked responses in more than 100 coeloconic sensilla in several dozen animals across most of the accessible antennal surface, using a panel of odorants that allowed us to identify unambiguously each sensilla type (ammonia for ac1, 1,4-diaminobutane for ac2, propanal and hexanol for ac3, and phenylacetaldehyde for ac4) (Yao et al., 2005) (Figure 4B, left). After electrophysiological identification, we noted the location of the sensilla on the antennal surface (Figure 4B, right).

This mapping process allowed a correlation of the electrophysiological and molecular properties of the coeloconic sensilla (Figure 4C). For example, ac1 sensilla were only detected in a region on the anterior antennal surface just ventral to the arista, and therefore most likely correspond to cluster A, containing *IR31a-IR75d-IR76b/IR92a*-expressing neurons. Our data fit well with the previous assignment of the *OR35a*-expressing neuron to the ac3 sensillum (Yao et al., 2005), which is found on the posterior of the antenna and is the only coeloconic sensillum class that unambiguously houses two neurons (Yao et al., 2005) (Figure 4B and data not shown). Although these results allow initial assignment of *IR*s to different coeloconic sensilla classes, we note that assignment of specific odor responses to individual *IR*-expressing OSNs is not possible from these data alone.

Glomerular Convergence of IR OSNs in the Antennal Lobe

All neurons expressing a given OR extend axons that converge upon a single antennal lobe glomerulus (Couto et al., 2005; Fishilevich and Vosshall, 2005), resulting in the representation of a cognate odor ligand as a spatially defined pattern of neural activity within the brain. To ask whether *IR*-expressing neurons have the same wiring logic, we investigated the targeting of OSNs expressing *IR76a* by constructing an *IR76a*-promoter GAL4 driver that recapitulates the endogenous expression pattern (Brand and Perrimon, 1993) (Figure 5A). Labeling of these neurons with mCD8:GFP revealed convergence of their axons on to a single glomerulus, ventral medial 4 (VM4), in the antennal lobe (Figure 5B). This glomerulus is one of approximately eight that was previously unaccounted for by maps of axonal projections of OR-expressing OSNs (Couto et al., 2005; Vosshall and Stocker, 2007).

IR Proteins Localize to Sensory Cilia

To determine where IRs localize in sensory neurons, we generated antibodies against IR25a. We detected broad expression of IR25a protein in sensory neurons of the arista, sacculus, and coeloconic sensilla (Figure 5C, left). All anti-IR25a immunoreactivity was abolished in an *IR25a* null mutant (Figure 5C, right). Low levels of IR25a could be detected in the axon segment adjacent to the cell body in some neurons, but no staining was observed along the axons as they entered the brain or at synapses within antennal lobe glomeruli (Figure 5D). In coeloconic neurons, prominent anti-IR25a staining was detected both in the cell body and in the distal tip of the dendrite, which corresponds to the ciliated outer dendritic segment innervating the sensory hair (Figure 5E). Relatively low levels were detected in the inner dendrites, suggesting the existence of a transport mechanism to concentrate receptor protein in cilia. A similar subcellular localization was observed in sacculus and aristal sensory neurons (Figures 5F and 5G). The specific targeting of an IR to sensory cilia suggests a role for these proteins in sensory detection.

Inducing Ectopic Olfactory Sensitivity by Misexpression of IRs

To test the hypothesis that IR genes encode chemosensory receptors, we investigated whether ectopic IR expression was sufficient to confer nonnative olfactory specificities. Three IRs expressed in ac4 sensilla (IR84a, IR76a, and IR75d) were individually misexpressed in ac3 sensilla with the *OR35a-GAL4* driver (Fishilevich and Vosshall, 2005). We used single-sensillum recordings to examine which, if any, of these three IRs could confer sensitivity to phenylacetaldehyde, the only known robust ligand for ac4 but not ac3 sensilla (Yao et al., 2005). Misexpression of IR84a conferred a strong response to phenylacetaldehyde (Figure 6A) that was not observed in control strains or in animals misexpressing either IR76a or IR75d (Figure 6B). Ectopically expressed IR84a did not confer sensitivity to the structurally related odor, phenylacetonitrile, which does not activate either ac3 or ac4 neurons (Yao et al., 2005). This indicates that misexpressed IR84a does not simply generate nonspecific ligand sensitivity in these neurons.

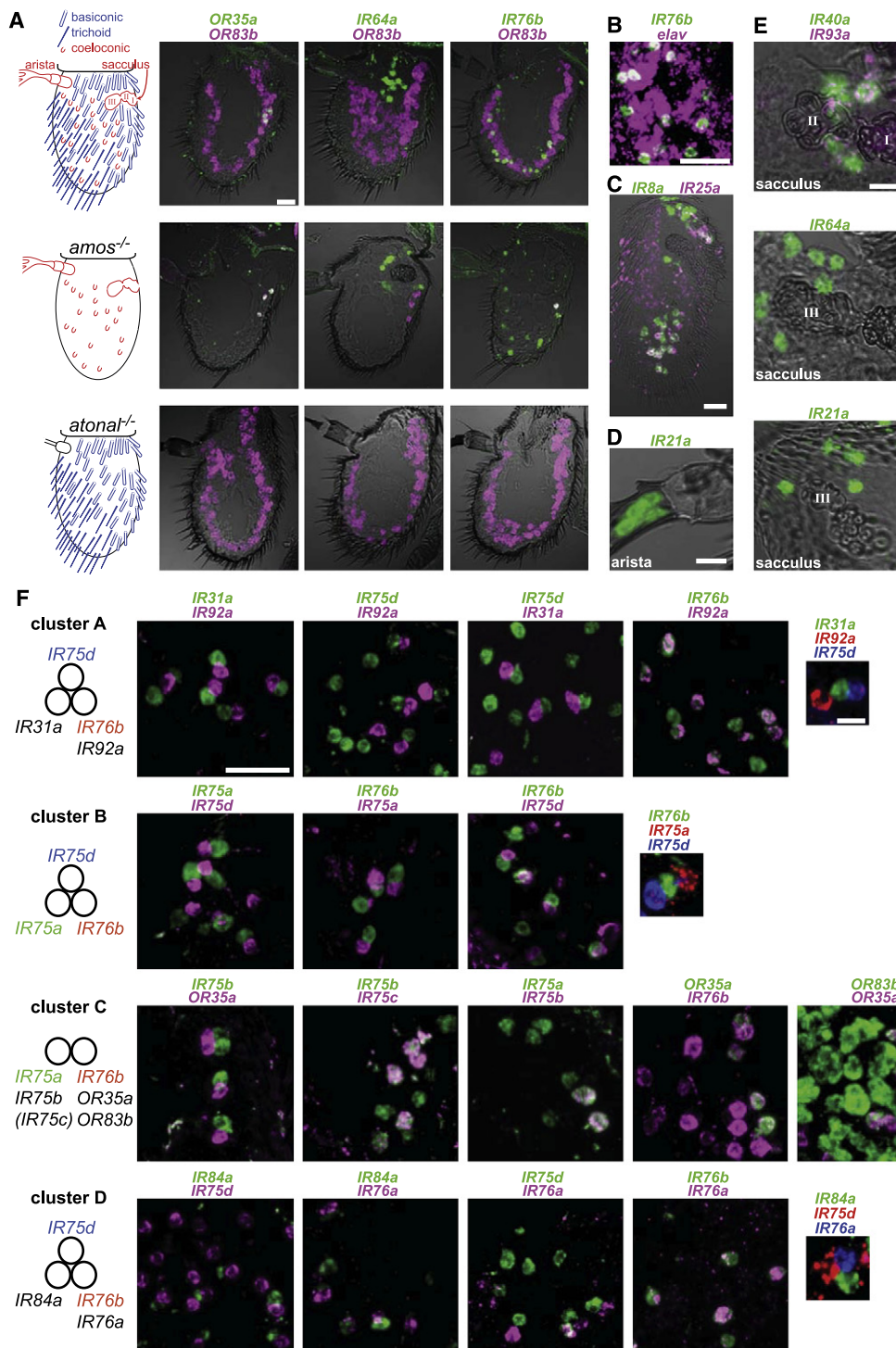We next compared the odor responses conferred by IR84a misexpression to the endogenous phenylacetaldehyde

Figure 3. A Topological Map of IR Expression in the Antenna

(A) Left: cartoons of the *Drosophila* antenna, in which sensory structures are color-coded by their developmental specification by the proneural genes *amos* (blue) or *atonal* (red). Right: two-color RNA in situ hybridization for *OR83b* (magenta) and *OR35a* (green, left), *IR64a* (green, middle), or *IR76b* (green, right) on antennal sections of wild-type (top), *amos* mutant (*amos¹/Df(2L)M36F-S6*) (middle), and *atonal* mutant (*ato¹/Df(3R)p13*) (bottom) animals. Scale bars represent 20 μm.

(B) Two-color RNA in situ hybridization for *IR76b* (green) and the neuronal marker *elav* (magenta) on a wild-type antennal section. The scale bar represents 20 μm.

(C) Two-color RNA in situ hybridization on an antennal section for *IR8a* (green) and *IR25a* (magenta). The scale bar represents 20 μm.

(D) One-color RNA in situ hybridization on an antennal section reveals expression of *IR21a* in the arista. The scale bar represents 10 μm.
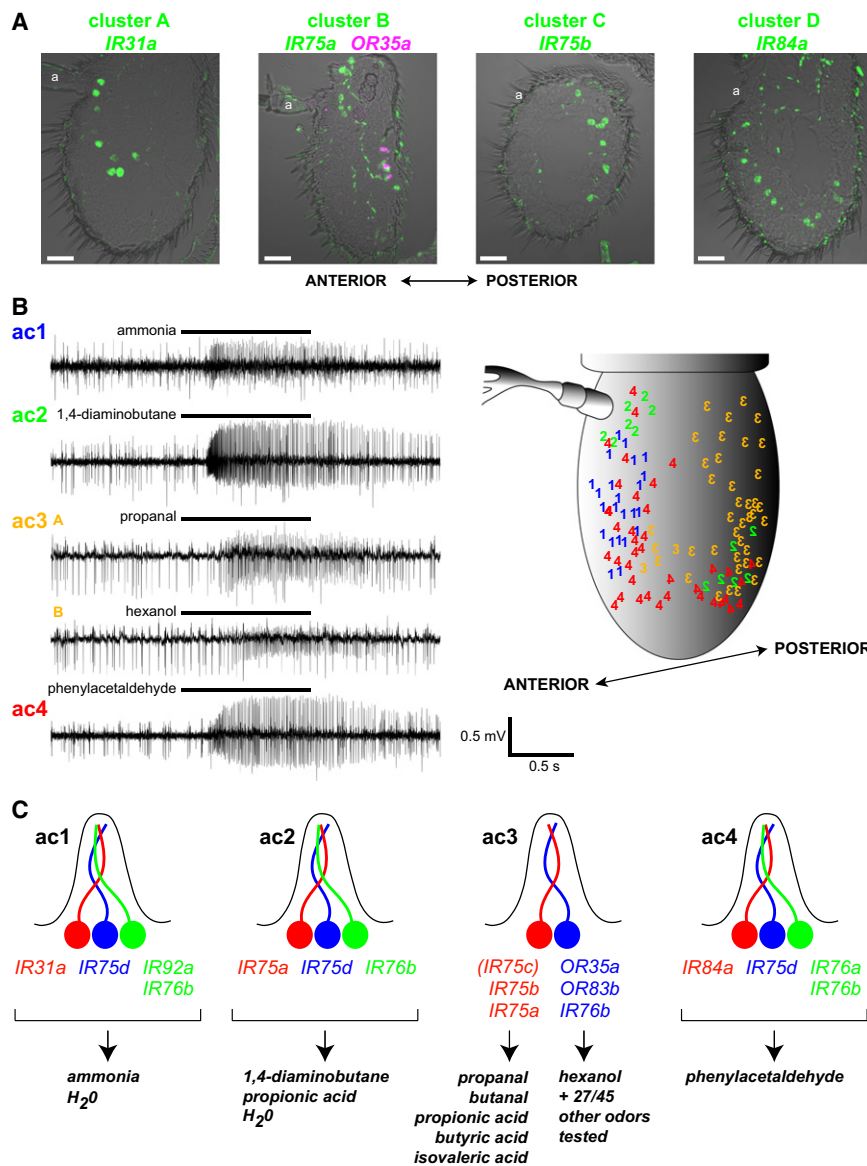
Figure 4. Integration of Molecular and Functional Maps in the Coeloconic Sensilla

(A) RNA in situ hybridization on antennal sections of wild-type animals for the indicated *IR* genes representing each of the four clusters. Cluster B is represented by *IR75a*-expressing OSNs (green) that are not paired with *OR35a*-expressing neurons (magenta). "a" indicates the position of the arista, which projects from the anterior surface of the antenna. Anterior is to the left in all images. Scale bars represent 20 μm.

(B) Left: representative traces of extracellular recordings of each coeloconic sensillum class, stimulated with diagnostic odorants (Yao et al., 2005) as indicated. Bars above the traces mark stimulus time (1 s). For ac3, two diagnostic odorants are shown, which specifically stimulate the A (large spike amplitude) or B (small spike amplitude) neuron. Right: Schematic of the topological distribution of ac1-ac4 coeloconic sensillum classes mapped manually after electrophysiological recordings from both the anterior and posterior surfaces of the antenna. Sensilla types are indicated as 1–4, with numbers reversed for sensilla on the posterior face of the antenna.

(C) Summary of the predicted molecular identity of *IR*-expressing neurons and sensilla classes they innervate. Best ligands (producing a response of >45 spikes/s) for each class are shown as the bottom, from a screen of a panel of 45 odors (Yao et al., 2005). All identified ligands of the ac3B *OR35a/OR83b/IR76b* neuron have been shown to be genetically dependent on *OR35a* (Yao et al., 2005).

6C and 6D), as subtraction of these values produces an IR84a-dependent phenylacetaldehyde dose-response curve that is statistically the same as that of ac4 sensilla (Figure 6E). Thus, misexpression of a single IR in ac3 is sufficient to confer an ectopic ligand- and receptor-specific odor sensitivity that is physiologically indistinguishable from endogenous responses.

To extend this analysis to a second IR, we examined whether misexpression of one of the *IR* genes uniquely expressed in ammonia-sensitive ac1 neurons (*IR31a* and *IR92a*) was sufficient to confer ectopic responsiveness to this odor. Because ac3 sensilla neurons display endogenous ammonia-evoked responses at modest stimulus concentrations, we used in these experiments the *IR76a*-promoter GAL4 transgene to misexpress

responses of ac4 sensilla by generating dose-response curves (Figures 6C and 6D). Stimulus-evoked spike frequencies of ac3 sensilla ectopically expressing IR84a are quantitatively very similar to those in ac4 sensilla, even exceeding the endogenous ac4 responses at higher odor concentrations (Figure 6D). These elevated responses are likely to be due to the contribution of weak endogenous phenylacetaldehyde responses that we observed in ac3 sensilla at high stimulus concentrations (Figures

(E) One- and two-color RNA in situ hybridization on antennal sections reveals coexpression of *IR40a* (green) and *IR93a* (magenta) in neurons surrounding the first and second chamber of the sacculus (top) and expression of *IR64a* (middle) and *IR21a* (bottom) in neurons surrounding the third chamber of the sacculus. The scale bar represents 10 μm.

(F) Two- and three-color RNA in situ hybridization for the indicated combinations of *IR* genes expressed in neurons in the main portion of the antenna. Pairwise comparison of physically adjacent neurons allows the definition of four distinct clusters (A–D) of *IR*-expressing neurons, summarized in the schemes on the left. *IR* genes expressed in more than one cluster are highlighted in color. The parentheses around *IR75c* refer to the expression of this gene in only a subset of cluster C (111 *IR75c*-expressing cells/155 *IR75b*-expressing cells = 71.6%). Scale bars in all two-color panels represent 20 μm, and scale bars in all three-color panels represent 5 μm.
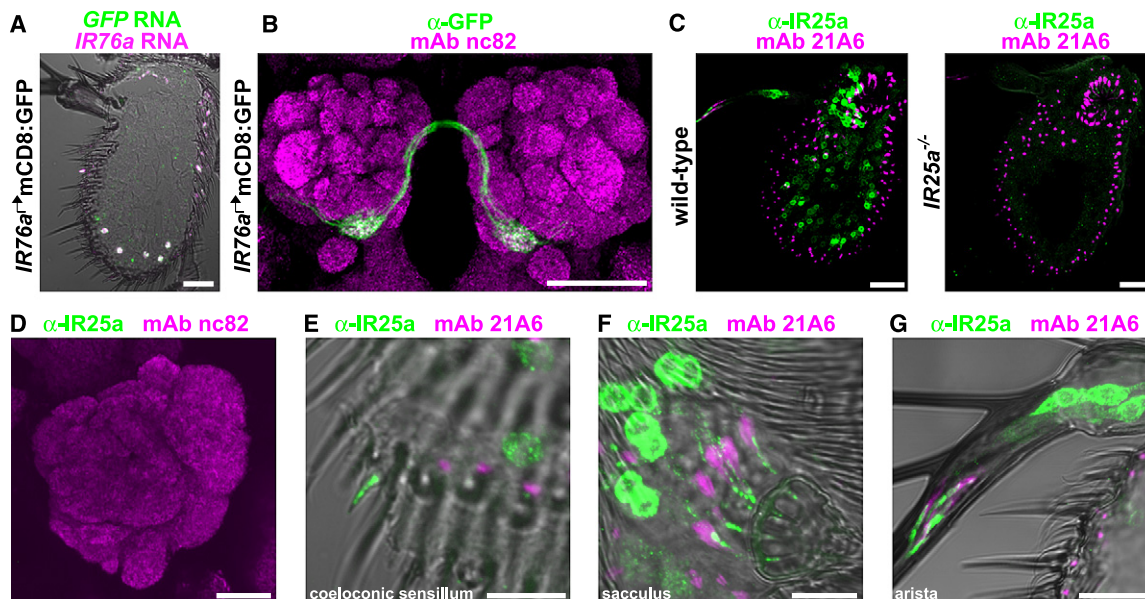
Figure 5. Glomerular Convergence of IR Axons and Ciliary Localization of IR Proteins

(A) Two-color RNA in situ hybridization for GFP (green) and *IR76a* (magenta) on an antennal section of an animal expressing the mCD8:GFP reporter under the control of the *IR76a* promoter-GAL4 driver (*IR76a promoter-GAL4/UAS-mCD8:GFP*). The scale bar represents 20 μm.

(B) Immunostaining of mCD8:GFP-labeled *IR76a* axon termini (anti-GFP, green) and neuropil (mAb nc82, magenta) on whole-mount brains of *IR76a promoter-GAL4/UAS-mCD8:GFP* animals. The scale bar represents 50 μm.

(C) Immunostaining for IR25a (green) and a cilia base marker (mAb 21A6, magenta) in antennal sections from wild-type (left) and *IR25a* null mutant (*IR25a^1^/IR25a^2^*) animals. Scale bars represent 20 μm.

(D) Immunostaining of IR25a (green) and neuropil (mAb nc82, magenta) in the antennal lobe of a wild-type animal. The scale bar represents 20 μm.

(E–G) High-magnification image of IR25a immunostaining (green) and cilia base immunostaining (mAb 21A6, magenta) in wild-type antennal sections illustrating IR25a cilia localization in a coeloconic neuron (E), sacculus neurons (F), and aristal neurons (G). Scale bars represent 10 μm.

these receptors in ammonia-insensitive ac4 sensilla (Figure 7A) (Yao et al., 2005). When *IR92a* was misexpressed in ac4 sensilla, these neurons became sensitive to stimulation by ammonia (Figures 7A and 7B). 1,4-diaminobutane, a control stimulus that does not activate either ac1 or ac4 neurons (Yao et al., 2005), did not stimulate ac4 sensilla misexpressing IR92a. Moreover, we did not observe nonspecific responses to ammonia in control UAS-*IR92a* animals or in animals in which a different receptor, *IR31a*, was misexpressed in ac4 OSNs (Figure 7B). We note that the magnitude of the ectopic IR92a ammonia response is lower than native ammonia-evoked responses of ac1 sensilla (Yao et al., 2005). This may be due to the lack of cofactors present in ac1 sensilla but not in ac4 sensilla. Nevertheless, these results suggest that IR92a comprises at least part of an ammonia-specific chemosensory receptor.

DISCUSSION

We present a characterization of the IRs, a family of iGluR-related proteins in *Drosophila*. The ligand-binding domains of IRs are divergent, and most lack known glutamate-binding residues, suggesting that they recognize distinct ligands. IRs are expressed in chemosensory neurons that do not express known insect chemosensory receptors, the ORs and GRs. Spatial patterns of IR gene expression correlate with known ligand sensitivities of these neurons. IR proteins concentrate in

the sensory cilia where chemical detection takes place. Misexpression analysis provides genetic evidence that the IRs function as chemosensory receptors. These receptors may define a molecular basis for *Drosophila* chemosensory modalities not linked to known receptor genes. Moreover, the IRs may reveal important evolutionary links in chemical detection mechanisms in diverse types of cells across prokaryotes and eukaryotes.

Molecular Biology of IR Function

The specific combinatorial expression patterns of IRs in sensory neurons and the diversity in their ligand-binding domains is difficult to rationalize with a general role in signal transduction, independent of ligand recognition. More importantly, the nonnative olfactory sensitivity induced by ectopic expression of *IR84a* and *IR92a* provides evidence that IR proteins function directly as ligand-specific chemosensory receptors. Although these experiments demonstrate a sufficiency of IRs for conferring odor responsiveness, definitive proof of their necessity will require analysis of loss-of-function mutations.

In animal nervous systems, iGluRs mediate neuronal communication by forming glutamate-gated ion channels (Mayer, 2006), and we speculate that IRs also form ion channels, gated by odors and other chemosensory stimuli. A growing number of ionotropic mechanisms in chemoreception are known. For example, members of the transient receptor potential (TRP) family of ion channels are the primary receptors for nociceptive compounds

including capsaicin and menthol (Jordt et al., 2003; Bandell et al., 2007) and have also been implicated in gustatory detection of acids (Huang et al., 2006; Ishimaru et al., 2006). Insect ORs also display functional properties of ion channels (Sato et al., 2008; Wicher et al., 2008). Proof that IRs function as ion channels will necessitate electrophysiological characterization of these receptors in heterologous expression systems, and evidence for direct binding of chemosensory ligands to IRs will require biochemical assays in vitro.

iGluRs normally function as heterotetrameric assemblies of variable subunit composition that exhibit differing functional properties such as ligand sensitivity and ion permeability. Our analysis indicates that up to five different IRs may be coexpressed in a single sensory neuron, raising the possibility that these receptors also form multimeric protein assemblies with subunit-dependent characteristics. Of particular interest are the two broadly expressed members of the family, IR8a and IR25a, which may represent common subunits in many different types of IR complexes. Their function is unclear, but it is possible that they have a coreceptor function with other IRs, analogous to that of OR83b (Larsson et al., 2004; Nakagawa et al., 2005; Benton et al., 2006; Sato et al., 2008). Preliminary analysis of *IR25a* mutants revealed no obvious defects in odor-evoked responses in coeloconic sensilla (data not shown), but this may be due to redundancy of IR25a with IR8a or the existence of homomeric IR receptors without IR8a or IR25a. Other IRs, such as IR75a and IR76b, are expressed in two or more types of coeloconic sensory neurons. In these cases, the response properties may be defined by the combination of *IR*s expressed in these distinct neuronal populations. However, the present lack of knowledge of relevant ligands for several coeloconic OSNs makes it difficult to match specific ligands to individual *IR* neurons on the basis of our expression map alone.

Comparative Chemosensation by IRs and ORs

The IR repertoire is remarkably similar in size, overall genomic organization, and sequence divergence to *Drosophila* ORs. Like the ORs, individual IRs are specifically expressed in small subpopulations of chemosensory neurons, and this expression is regulated by relatively short (<1–2 kb) upstream regulatory regions (Couto et al., 2005; Fishilevich and Vosshall, 2005; Ray et al., 2007) (Figures 5A and 5B; and R.B., unpublished data). Furthermore, at least one population of *IR*-expressing neurons converges on to a single glomerulus in the antennal lobe, similar to the wiring logic established for OR-expressing neurons both in invertebrate and vertebrate olfactory systems (Mombaerts et al., 1996; Gao et al., 2000; Vosshall et al., 2000; Couto et al., 2005; Fishilevich and Vosshall, 2005). Some differences are observed, however, in the organizational logic of IR and OR expression. Most OR-expressing neurons express a single OR gene, along with OR83b, in distinct clusters that innervate specific olfactory sensilla. In contrast, many IR-expressing neurons identified in the antenna express two or three IR genes, in addition to one or both of the broadly expressed *IR8a* and *IR25a* genes. Moreover, overlap is observed both between the molecular composition of different IR neurons and the combination of neurons that innervate a given sensillum. For example, *IR76b* is coexpressed with at least two other different IR genes in at least two different

sensilla—with *IR92a* in ac1 and with *IR76a* in ac4—as well as being coexpressed with *OR35a* and *OR83b* in ac3. Although the precise biological logic of IR coexpression awaits the matching of specific chemosensory ligands to IR-expressing neurons, combinatorial expression of IRs may contribute more significantly to their role in sensory detection than for ORs.

Why does *Drosophila* possess two types of antennal chemosensory receptors? Although both may be ionotropic, IRs and ORs are not simply slight evolutionary variants. The receptor families are molecularly unrelated, are under the control of distinct developmental programs, and are housed within sensory structures of radically different morphology. Thus, it seems likely that these chemosensory receptors fulfill distinct functions in chemosensation. Analysis of the chemosensory behaviors mediated by IR sensory circuits—now possible with our identification of specific molecular markers for these pathways—may provide insights into the contributions of these different olfactory subsystems. IRs may also have functions in other chemosensory modalities, as two antennal IRs are also detected in the proboscis, and the expression of 46 members of the repertoire remains unknown.

An Evolutionarily Ancient Chemical-Sensing Mechanism

Chemosensation is an ancient sensory modality that predates the evolution of the eukaryotes. Are there traces of conservation in the molecular mechanism by which prokaryotes and eukaryotes sense external chemicals? iGluRs have long been recognized to have prokaryotic origins. Their ion channel domain is homologous to bacterial potassium channels, and the ligand binding domain is structurally related to bacterial periplasmic binding proteins (PBPs), extracellular proteins that scavenge or sense amino acids, carbohydrates, and metal ions by coupling to transporters or chemotaxis receptors (Mayer and Armstrong, 2004; Mayer, 2006). Evolutionary connections between iGluRs and PBP function have not often been considered, perhaps in part because of their very weak primary sequence similarity, the widespread occurrence of the PBP fold—also present, for example, in bacterial transcription regulators—and the dedicated role for iGluRs in mediating or regulating synaptic transmission, a process seemingly distant from bacterial solute uptake and chemotaxis.

Our discovery of a family of divergent iGluR-like proteins that may act as peripheral chemosensors provides a link between the disparate functions of these protein modules. Although a role for IRs in detecting diverse external ligands is analogous to the function of bacterial PBPs, the primary sequence and neuronal expression of IRs is clearly closer to the properties of iGluRs. Intriguingly, a large family of iGluR-related proteins, the GLRs, has also been identified in the plant *Arabidopsis thaliana* (Lam et al., 1998; Chiu et al., 1999). Almost nothing is known about their physiological functions, but bioinformatic analysis of GLRs suggests that glutamate is unlikely to be their natural ligand (Dubos et al., 2003; Qi et al., 2006). It is possible that GLRs may have roles as chemosensors, for example in detection of soil nutrients or airborne volatiles. Thus, although iGluRs have been intensely studied for their roles in synaptic communication, our characterization of the IRs leads us to suggest that the ancestral function of this protein family may have been in
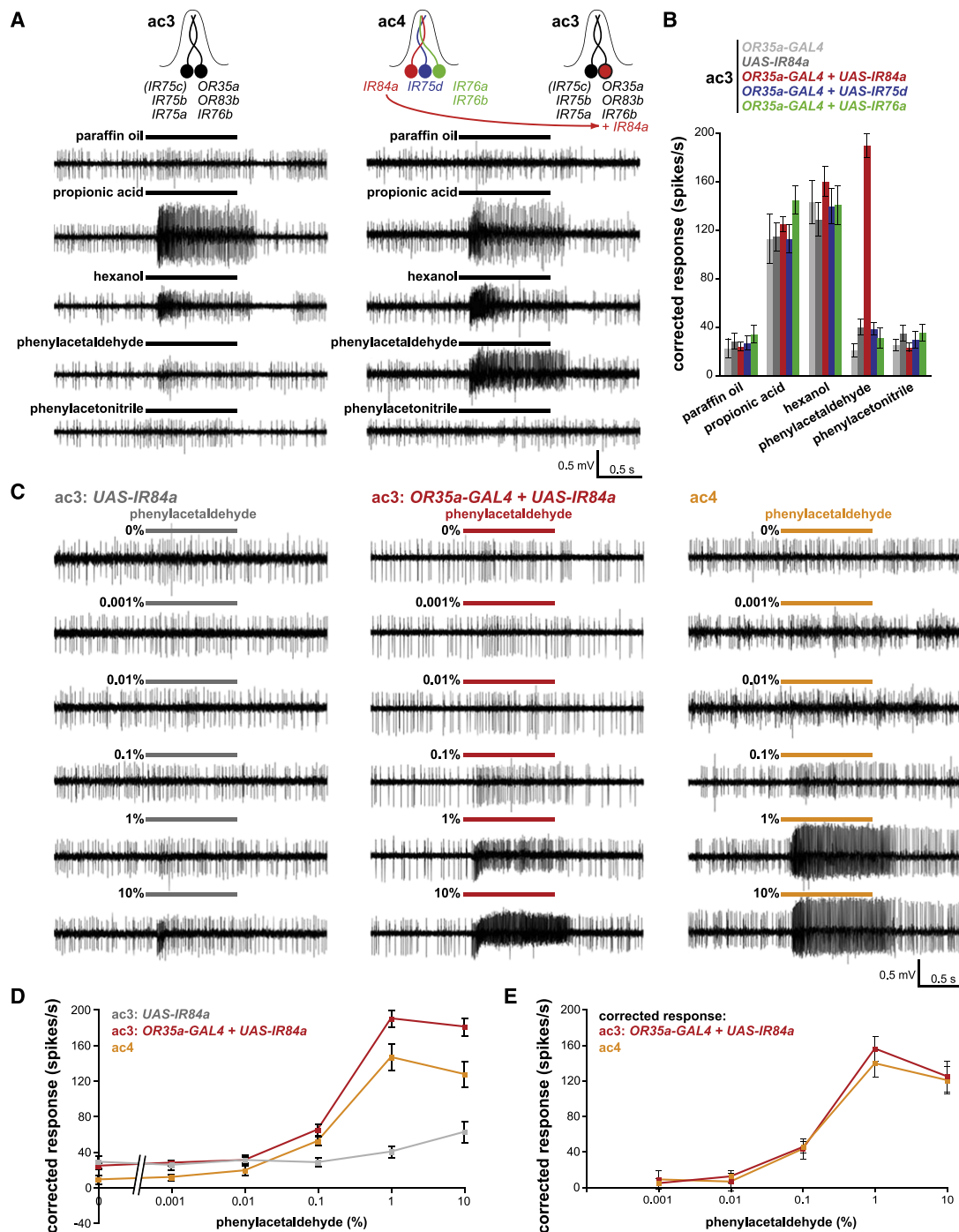
Figure 6. IR84a Misexpression Confers Ectopic Olfactory Sensitivity to Phenylacetaldehyde

(A) Representative traces of extracellular recordings of neuronal responses to the indicated stimuli in control ac3 sensilla (*UAS-IR84a*/+) (left) and in ac3 sensilla in which *IR84a* is misexpressed in *OR35a* neurons (*UAS-IR84a*/+;*OR35a-GAL4*/+) (right). Bars above the traces mark stimulus time (1 s). For these experiments, all odors were used at 1% concentration except for hexanol, which was diluted to 0.001%.

(B) Quantification of mean odor responses (±SEM; n = 8–16, male flies) of the five indicated genotypes (*OR35a-GAL4*/+ [light gray], *UAS-IR84a*/+ [dark gray], *UAS-IR84a*/+;*OR35a-GAL4*/+ [red], *UAS-IR75d*/+;*OR35a-GAL4*/+) [blue], and *UAS-IR76a*/+;*OR35a-GAL4*/+ [green]), to the indicated stimuli; concentrations as described in (A). Responses of ac3 sensilla neurons to paraffin oil, propionic acid, hexanol, and phenylacetonitrile are not significantly different between genotypes (ANOVA; p > 0.1657), whereas responses to phenylacetaldehyde are significantly different in sensilla ectopically expressing *IR84a* compared to the other genotypes (ANOVA with post hoc t tests; p < 0.0001).

(C) Representative traces of extracellular recordings of neuronal responses to the indicated dilution of phenylacetaldehyde in control ac3 sensilla (*UAS-IR84a*/+) (left), in ac3 sensilla in animals in which *IR84a* is misexpressed in *OR35a* neurons (*UAS-IR84a*/+;*OR35a-GAL4*/+) (middle), and in ac4 sensilla from

Figure 7. IR92a Misexpression Confers Ectopic Olfactory Sensitivity to Ammonia

(A) Representative traces of extracellular recordings of neuronal responses to the indicated stimuli in wild-type ac4 sensilla (left) and in ac4 sensilla in animals in which *IR92a* (middle) or *IR31a* (right) from ac1 sensilla are misexpressed in *IR76a*-expressing ac4 neurons (*IR76a*-GAL4/UAS-*IR92a* and *IR76a*-GAL4/UAS-*IR31a*, respectively). Bars above the traces mark stimulus time (1 s).

(B) Quantification of mean responses to the stimuli indicated for the four genotypes (±SEM; n = 9–10, male flies). Responses of ac4 sensilla to paraffin oil, water, phenylacetaldehyde (1%) and 1,4-diaminobutane (10%) are not significantly different between genotypes (ANOVA; p > 0.3044), whereas responses to ammonia (10%) are significantly different in flies ectopically expressing *IR92a* (ANOVA with post hoc t tests; p < 0.0001).

detecting diverse chemical ligands to mediate both intercellular communication and environmental chemical sensing.

EXPERIMENTAL PROCEDURES

Bioinformatics
Gene Identification
IR genes were identified by exhaustive searches of the *Drosophila* genome with TBLASTN and PSI-BLAST (Altschul et al., 1997). We used the iGluR-related genes that emerged from our comparative genomics screen (Benton et al., 2007) as initial queries to identify related genes, which were then used as queries in further searches in an iterative process until no new sequences were identified. Membrane topology and domain structure predictions of IR protein sequences were examined with SignalP 3.0 (Bendtsen et al., 2004), TMHMM 2.0 (Krogh et al., 2001), and SMART (Schultz et al., 1998). CG14586 encodes two tandem ion channel domains, which we considered to be a likely computational misprediction and reannotated as two separate genes, each encoding a single ion channel domain (noted in Figure 1A as

---

UAS-IR84a/+;OR35a-GAL4/+ animals (right). ac3 sensilla were unambiguously identified by their responses to propionic acid and hexanol (see [A] and [B]). Bars above the traces mark stimulus time (1 s).

(D) Quantification of mean responses to the phenylacetaldehyde stimuli indicated for the three genotypes shown in (C) (±SEM; n = 10–16, male flies). At 0.1% phenylacetaldehyde, the ac3 + IR84a and ac4 responses are both significantly higher than the control ac3 sensilla (ANOVA with post hoc t tests; p < 0.0008); at 1% and 10%, the ac3 + IR84a sensilla responses are significantly higher than ac4 (ANOVA with post hoc t tests; p < 0.0001).

(E) Plot of dose-responses curves of data shown in (D), in which the ac4 sensilla phenylacetaldehyde responses have been corrected for the paraffin oil response, and the phenylacetaldehyde responses of ac3 + IR84a sensilla have been corrected for both paraffin oil responses and endogenous weak ac3 phenylacetaldehyde responses (gray values in [D]). The curves are not significantly different at any stimulus concentration (ANOVA; p = 0.6629).

CG14586-A, CG14586-B). Experimental support for the existence of two distinct transcription units is provided by our observation that RNA in situ hybridization with a probe for IR75c (CG14586-A) highlights only a subset of cells labeled by a probe for IR75b (CG14586-B) (Figure 3F). For most *IR*s, verification of the computationally predicted protein sequences awaits isolation of full-length cDNAs. Thus, the phylogenetic relationships illustrated in Figure 1B and sequence alignments in Figure 1C and Figure 2 should not be considered definitive.

Gene Nomenclature
Identified genes were named by applying the same conventions adopted for the *OR* and *GR* gene families (*Drosophila* Odorant Receptor Nomenclature Committee, 2000). In brief, genes are named according to their location within one of the 102 primary numbered cytogenetic units of the *Drosophila* genome. Where there is only one candidate receptor within a given numbered region, it is appended with a lowercase "a"; where there are multiple receptors within a region, these are supplied with lowercase letters as a unique identifier according to their relative position on the cytogenetic map.

Sequence Alignments and Phylogenetic Analysis
Alignments of specific domains of iGluRs/IRs were generated with ClustalW, with manual adjustments, and were visualized in Jalview (Clamp et al., 2004). The phylogenetic tree was generated by aligning full length sequences with PROBCONS (Do et al., 2005) and tree inference with RAxML (Stamatakis, 2006). The tree was viewed with FigTree v1.1.2.

Molecular Biology
For RT-PCR analysis of *IR* expression, cDNA was synthesized from *Drosophila* tissues with the Absolutely RNA Microprep Kit (Stratagene) and Superscript First-Strand Synthesis System (Invitrogen). Gene-specific primers for PCR were designed with Primer3 (http://frodo.wi.mit.edu/cgi-bin/primer3/primer3_www.cgi/) to amplify ~500 bp spanning, where possible, at least one intron. Primer pairs were verified for their ability to amplify products from genomic DNA with Taq DNA polymerase (Invitrogen). DNA templates for antisense probe synthesis were generated by T:A cloning cDNA or genomic PCR products for each *IR* gene into pGEM-T Easy (Promega). Antisense Digoxygenin (DIG)-, Fluorescein-, or Biotin-labeled RNA probes were synthesized via standard methods. Details of transgene construction are provided in the Supplemental Data available online.

Drosophila Stocks
Drosophila stocks were maintained on conventional cornmeal-agar-molasses medium under a 12 hr light:12 hr dark cycle at 25°C. Oregon-R was used as a wild-type control. Previously described mutant alleles and transgenic lines used are listed in the Supplemental Data. Transgenic lines were generated in this study by Genetic Services Inc. (Cambridge, MA) with either P-element-mediated transformation or, for *UAS-IR84a*, the phiC31-based integration system (Bischof et al., 2007). Gene targeting of *IR25a* was performed essentially as described (Larsson et al., 2004), with nine independent insertions of the targeting construct. From approximately 150,000 F2 progeny, two null mutants were obtained, which were confirmed by PCR on genomic DNA preparations from homozygous mutant animals.

Histology and Immunocytochemistry
In situ RNA hybridization was performed essentially as described (Fishilevich and Vosshall, 2005) with combinations of Fluorescein-, DIG-, and Biotin-labeled RNA probes, which were visualized with the TSA Plus Fluorescein, Cy5, or Cy3 Fluorescence Systems (Perkin Elmer), respectively. Immunofluorescence on antennal sections or whole-mount brains was performed as described (Benton et al., 2006). Previously described antibodies are listed in the Supplemental Data. Rabbit polyclonal antibodies against IR25a were raised against the synthetic peptides SKAALRPRFNQYPATFKPRF and DVAEANAERSNAADHPGKLVDGV and affinity-purified by Proteintech Group, Inc (Chicago) and used at 1:1000.

Electrophysiology and Odorants
Extracellular recordings in single sensilla of 2- to 8-day-old flies were performed as described (Jones et al., 2007). Odorants were obtained from Sigma-Aldrich at high purity. Chemical Abstracts Service (CAS) numbers are as follows: aqueous ammonia (ammonium hydroxide) (1336-21-6), 1,4-diaminobutane (110-60-1), propanal (123-38-6), hexanol (111-27-3), propionic acid (79-09-4), phenylacetaldehyde (122-78-1), and phenylacetonitrile (140-29-4). Odors were used at 1% (v/v in solvent) unless indicated otherwise in the figures, diluted either in paraffin oil (propanal, hexanol, phenylacetaldehyde, phenylacetonitrile) or water (ammonium hydroxide, propionic acid, 1,4-diaminobutane). The onset of odor responses varied slightly (usually <200 ms) between animals of the same genotype recorded on different days, most likely because of small variations in the position of the odor delivery apparatus relative to the preparation. For quantification of responses, we determined the time of onset of the response of a control wild-type sensillum to either propionic acid (for ac3) or phenylacetaldehyde (for ac4) for each recording session. Corrected responses for all recordings in the same session were quantified by counting spikes in a 0.5 s window from this time point, subtracting the number of spontaneous spikes in a 0.5 s window prior to stimulation, and doubling the result to obtain spikes/s. We summed spikes from all neurons in a given sensillum because of difficulties in reliable spike sorting in coeloconic sensilla (Yao et al., 2005). After verifying that responses were normally distributed, we compared all genotypes for a given stimulus by ANOVA, with genotype as the main effect, followed by post hoc t tests.

SUPPLEMENTAL DATA

Supplemental Data include Supplemental Experimental Procedures and can be found with this article online at http://www.cell.com/supplemental/S0092-8674(08)01561-4.

REFERENCES

Altschul, S.F., Madden, T.L., Schaffer, A.A., Zhang, J., Zhang, Z., Miller, W., and Lipman, D.J. (1997). Gapped BLAST and PSI-BLAST: a new generation of protein database search programs. Nucleic Acids Res. *25*, 3389–3402.

Armstrong, N., and Gouaux, E. (2000). Mechanisms for activation and antagonism of an AMPA-sensitive glutamate receptor: crystal structures of the GluR2 ligand binding core. Neuron *28*, 165–181.

Armstrong, N., Sun, Y., Chen, G.Q., and Gouaux, E. (1998). Structure of a glutamate-receptor ligand-binding core in complex with kainate. Nature *395*, 913–917.

Bandell, M., Macpherson, L.J., and Patapoutian, A. (2007). From chills to chilis: mechanisms for thermosensation and chemesthesis via thermoTRPs. Curr. Opin. Neurobiol. *17*, 490–497.

Bargmann, C.I. (2006). Comparative chemosensation from receptors to ecology. Nature *444*, 295–301.

Bendtsen, J.D., Nielsen, H., von Heijne, G., and Brunak, S. (2004). Improved prediction of signal peptides: SignalP 3.0. J. Mol. Biol. *340*, 783–795.

Benton, R. (2008). Chemical sensing in *Drosophila*. Curr. Opin. Neurobiol. *18*, 357–363.

Benton, R., Sachse, S., Michnick, S.W., and Vosshall, L.B. (2006). Atypical membrane topology and heteromeric function of *Drosophila* odorant receptors *in vivo*. PLoS Biol. *4*, e20.

Benton, R., Vannice, K.S., and Vosshall, L.B. (2007). An essential role for a CD36-related receptor in pheromone detection in *Drosophila*. Nature *450*, 289–293.

Bischof, J., Maeda, R.K., Hediger, M., Karch, F., and Basler, K. (2007). An optimized transgenesis system for *Drosophila* using germ-line-specific phiC31 integrases. Proc. Natl. Acad. Sci. USA *104*, 3312–3317.

Brand, A.H., and Perrimon, N. (1993). Targeted gene expression as a means of altering cell fates and generating dominant phenotypes. Development *118*, 401–415.

Chiu, J., DeSalle, R., Lam, H., Meisel, L., and Coruzzi, G. (1999). Molecular evolution of glutamate receptors: a primitive signaling mechanism that existed before plants and animals diverged. Mol. Biol. Evol. *16*, 826–838.

Clamp, M., Cuff, J., Searle, S.M., and Barton, G.J. (2004). The Jalview Java alignment editor. Bioinformatics *20*, 426–427.

Couto, A., Alenius, M., and Dickson, B.J. (2005). Molecular, anatomical, and functional organization of the *Drosophila* olfactory system. Curr. Biol. *15*, 1535–1547.

Dahanukar, A., Hallem, E., and Carlson, J. (2005). Insect chemoreception. Curr. Opin. Neurobiol. *15*, 423–430.

Do, C.B., Mahabhashyam, M.S., Brudno, M., and Batzoglou, S. (2005). Prob-Cons: Probabilistic consistency-based multiple sequence alignment. Genome Res. *15*, 330–340.

Dohlman, H.G. (2002). G proteins and pheromone signaling. Annu. Rev. Physiol. *64*, 129–152.

Drosophila Odorant Receptor Nomenclature Committee. (2000). A unified nomenclature system for the *Drosophila* odorant receptors. Cell *102*, 145–146.

Dubos, C., Huggins, D., Grant, G.H., Knight, M.R., and Campbell, M.M. (2003). A role for glycine in the gating of plant NMDA-like receptors. Plant J. *35*, 800–810.

Fishilevich, E., and Vosshall, L.B. (2005). Genetic and functional subdivision of the *Drosophila* antennal lobe. Curr. Biol. *15*, 1548–1553.

Gao, Q., Yuan, B., and Chess, A. (2000). Convergent projections of *Drosophila* olfactory neurons to specific glomeruli in the antennal lobe. Nat. Neurosci. *3*, 780–785.

Goulding, S.E., zur Lage, P., and Jarman, A.P. (2000). *amos*, a proneural gene for *Drosophila* olfactory sense organs that is regulated by *lozenge*. Neuron *25*, 69–78.

Gupta, B.P., and Rodrigues, V. (1997). Atonal is a proneural gene for a subset of olfactory sense organs in Drosophila. Genes Cells *2*, 225–233.

Huang, A.L., Chen, X., Hoon, M.A., Chandrashekar, J., Guo, W., Trankner, D., Ryba, N.J., and Zuker, C.S. (2006). The cells and logic for mammalian sour taste detection. Nature *442*, 934–938.

Ishimaru, Y., Inada, H., Kubota, M., Zhuang, H., Tominaga, M., and Matsunami, H. (2006). Transient receptor potential family members PKD1L3 and PKD2L1 form a candidate sour taste receptor. Proc. Natl. Acad. Sci. USA *103*, 12569–12574.

Jhaveri, D., Sen, A., Reddy, G.V., and Rodrigues, V. (2000). Sense organ identity in the *Drosophila* antenna is specified by the expression of the proneural gene *atonal*. Mech. Dev. *99*, 101–111.

Jin, R., Banke, T.G., Mayer, M.L., Traynelis, S.F., and Gouaux, E. (2003). Structural basis for partial agonist action at ionotropic glutamate receptors. Nat. Neurosci. *6*, 803–810.

Jones, W.D., Cayirlioglu, P., Kadow, I.G., and Vosshall, L.B. (2007). Two chemosensory receptors together mediate carbon dioxide detection in *Drosophila*. Nature *445*, 86–90.

Jordt, S.E., McKemy, D.D., and Julius, D. (2003). Lessons from peppers and peppermint: the molecular logic of thermosensation. Curr. Opin. Neurobiol. *13*, 487–492.

Krogh, A., Larsson, B., von Heijne, G., and Sonnhammer, E.L. (2001). Predicting transmembrane protein topology with a hidden Markov model: application to complete genomes. J. Mol. Biol. *305*, 567–580.

Lam, H.M., Chiu, J., Hsieh, M.H., Meisel, L., Oliveira, I.C., Shin, M., and Coruzzi, G. (1998). Glutamate-receptor genes in plants. Nature *396*, 125–126.

Larsson, M.C., Domingos, A.I., Jones, W.D., Chiappe, M.E., Amrein, H., and Vosshall, L.B. (2004). *Or83b* encodes a broadly expressed odorant receptor essential for *Drosophila* olfaction. Neuron *43*, 703–714.

Littleton, J.T., and Ganetzky, B. (2000). Ion channels and synaptic organization: analysis of the *Drosophila* genome. Neuron *26*, 35–43.

Lundin, C., Käll, L., Kreher, S.A., Kapp, K., Sonnhammer, E.L., Carlson, J.R., von Heijne, G., and Nilsson, I. (2007). Membrane topology of the *Drosophila* OR83b odorant receptor. FEBS Lett. *581*, 5601–5604.

Mayer, M.L. (2005). Crystal structures of the GluR5 and GluR6 ligand binding cores: molecular mechanisms underlying kainate receptor selectivity. Neuron *45*, 539–552.

Mayer, M.L. (2006). Glutamate receptors at atomic resolution. Nature *440*, 456–462.

Mayer, M.L., and Armstrong, N. (2004). Structure and function of glutamate receptor ion channels. Annu. Rev. Physiol. *66*, 161–181.

Mayer, M.L., Ghosal, A., Dolman, N.P., and Jane, D.E. (2006). Crystal structures of the kainate receptor GluR5 ligand binding core dimer with novel GluR5-selective antagonists. J. Neurosci. *26*, 2852–2861.

Mombaerts, P., Wang, F., Dulac, C., Chao, S.K., Nemes, A., Mendelsohn, M., Edmondson, J., and Axel, R. (1996). Visualizing an olfactory sensory map. Cell *87*, 675–686.

Nakagawa, T., Sakurai, T., Nishioka, T., and Touhara, K. (2005). Insect sex-pheromone signals mediated by specific combinations of olfactory receptors. Science *307*, 1638–1642.

Naur, P., Hansen, K.B., Kristensen, A.S., Dravid, S.M., Pickering, D.S., Olsen, L., Vestergaard, B., Egebjerg, J., Gajhede, M., Traynelis, S.F., and Kastrup, J.S. (2007). Ionotropic glutamate-like receptor delta2 binds D-serine and glycine. Proc. Natl. Acad. Sci. USA *104*, 14116–14121.

Qi, Z., Stephens, N.R., and Spalding, E.P. (2006). Calcium entry mediated by GLR3.3, an *Arabidopsis* glutamate receptor with a broad agonist profile. Plant Physiol. *142*, 963–971.

Ray, A., van Naters, W.G., Shiraiwa, T., and Carlson, J.R. (2007). Mechanisms of odor receptor gene choice in *Drosophila*. Neuron *53*, 353–369.

Sato, K., Pellegrino, M., Nakagawa, T., Nakagawa, T., Vosshall, L.B., and Touhara, K. (2008). Insect olfactory receptors are heteromeric ligand-gated ion channels. Nature *452*, 1002–1006.

Schultz, J., Milpetz, F., Bork, P., and Ponting, C.P. (1998). SMART, a simple modular architecture research tool: identification of signaling domains. Proc. Natl. Acad. Sci. USA *95*, 5857–5864.

Scott, K., Brady, R., Jr., Cravchik, A., Morozov, P., Rzhetsky, A., Zuker, C., and Axel, R. (2001). A chemosensory gene family encoding candidate gustatory and olfactory receptors in *Drosophila*. Cell *104*, 661–673.

Stamatakis, A. (2006). RAxML-VI-HPC: maximum likelihood-based phylogenetic analyses with thousands of taxa and mixed models. Bioinformatics *22*, 2688–2690.

Vosshall, L.B., Amrein, H., Morozov, P.S., Rzhetsky, A., and Axel, R. (1999). A spatial map of olfactory receptor expression in the *Drosophila* antenna. Cell *96*, 725–736.

Vosshall, L.B., and Stocker, R.F. (2007). Molecular architecture of smell and taste in *Drosophila*. Annu. Rev. Neurosci. *30*, 505–533.

Vosshall, L.B., Wong, A.M., and Axel, R. (2000). An olfactory sensory map in the fly brain. Cell *102*, 147–159.

Wicher, D., Schafer, R., Bauernfeind, R., Stensmyr, M.C., Heller, R., Heinemann, S.H., and Hansson, B.S. (2008). *Drosophila* odorant receptors are both ligand-gated and cyclic-nucleotide-activated cation channels. Nature *452*, 1007–1011.

Wistrand, M., Kall, L., and Sonnhammer, E.L. (2006). A general model of G protein-coupled receptor sequences and its application to detect remote homologs. Protein Sci. *15*, 509–521.

Yao, C.A., Ignell, R., and Carlson, J.R. (2005). Chemosensory coding by neurons in the coeloconic sensilla of the *Drosophila* antenna. J. Neurosci. *25*, 8359–8367.

zur Lage, P.I., Prentice, D.R., Holohan, E.E., and Jarman, A.P. (2003). The *Drosophila* proneural gene *amos* promotes olfactory sensillum formation and suppresses bristle formation. Development *130*, 4683–4693.